1-1-2012

Holocene subsurface temperature variability in the eastern Antarctic continental margin

J H Kim

X Crosta

V Willmott

H Renssen

J Bonnin

See next page for additional authors

Authors

J H Kim, X Crosta, V Willmott, H Renssen, J Bonnin, Peer Helmke, S Schouten, and J S Sinninghe Damste

Holocene subsurface temperature variability in the eastern Antarctic continental margin

Jung-Hyun Kim,[1] Xavier Crosta,[2] Veronica Willmott,[1,3] Hans Renssen,[4] Jérôme Bonnin,[2] Peer Helmke,[5] Stefan Schouten,[1] and Jaap S. Sinninghe Damsté[1]

[1]   We reconstructed subsurface ($\sim$45–200 m water depth) temperature variability in the eastern Antarctic continental margin during the late Holocene, using an archaeal lipid-based temperature proxy (TEX_{86}^L). Our results reveal that subsurface temperature changes were probably positively coupled to the variability of warmer, nutrient-rich Modified Circumpolar Deep Water (MCDW, deep water of the Antarctic circumpolar current) intrusion onto the continental shelf. The TEX_{86}^L record, in combination with previously published climatic records, indicates that this coupling was probably related to the thermohaline circulation, seasonal variability in sea ice extent, sea temperature, and wind associated with high frequency climate dynamics at low-latitudes such as internal El Niño Southern Oscillation (ENSO). This in turn suggests a linkage between centennial ENSO-like variability at low-latitudes and intrusion variability of MCDW into the eastern Antarctic continental shelf, which might have further impact on ice sheet evolution. **Citation:**   Kim, J.-H., X. Crosta, V. Willmott, H. Renssen, J. Bonnin, P. Helmke, S. Schouten, and J. S. Sinninghe Damsté (2012), Holocene subsurface temperature variability in the eastern Antarctic continental margin, *Geophys. Res. Lett.*, *39*, L06705, doi:10.1029/2012GL051157.

1.   Introduction

[2]   An important clue towards the potential future impact of Antarctic warming on glaciological changes can be obtained from past temperature records beyond the instrumental period. To properly address Antarctic's climate variability and its relationship to the global climate system in relation to natural forcing, it is essential to investigate temperature records beyond the instrumental period. The number of Holocene quantitative temperature records from ice cores [*Stenni et al.*, 2010], from the southern hemisphere (SH) mid-latitude [*Hodell et al.*, 2001; *Bianchi and Gersonde*, 2004; *Nielsen et al.*, 2004; *Kaiser et al.*, 2008], and from the continental margin of the western Antarctic Peninsula [*Shevenell et al.*, 2011] has increased substantially in recent years. However, quantitative temperature records from the eastern Antarctic continental margin are still lacking since reconstructions based on diatom-based transfer

functions, one of the most widely used techniques in the Southern Ocean to decipher sea surface temperature (SST), are not sensitive enough for quantitative temperature reconstruction for the coastal Antarctic [*Crosta et al.*, 2008]. Here we overcome this obstacle by applying an archaeal membrane lipid-based paleothermometer (TEX_{86}^L) for the Polar Oceans [*Kim et al.*, 2010], a modified version of the initial TEX_{86} [*Schouten et al.*, 2002], to estimate ocean temperatures in the eastern Antarctic continental margin.

2.   Material and Methods

[3]   We obtained Holocene climate records from piston core MD03-2601 (66°03.07S; 138°33.43E; 746 m water depth, Figure 1), recovered from the slope of one of the depressions composing the Dumont d'Urville Trough off Adélie Land retrieved during the MD130 Images X cruise (CADO-Coring Adélie Diatom Oozes) with R.V. Marion Dufresne II [*Denis et al.*, 2009]. The Dumont d'Urville Trough is located along the East Antarctic coast in the eastern Indian sector of the Southern Ocean (see Figure S1 in the auxiliary material).[1] This area is influenced by several water masses and currents [*Bindoff et al.*, 2000; *Lacarra et al.*, 2011; *Williams et al.*, 2010]: (1) the wind-driven East Wind Drift, also called Antarctic Coastal Current, which flows westward and transports Antarctic Surface Water that can be subdivided into Summer Surface Water and Winter Water; (2) the MCDW at depths of $\sim$200–800 m, which intrudes onto the shelf region and provides a reservoir of nutrient-rich, warmer water that subsequently upwells into the upper water column; and (3) the High Salinity Shelf Water, formed by brine-rejection during winter sea ice formation and cooling of the MCDW, which flows northward as part of the Adélie Land Bottom Water. The age model of the core [*Denis et al.*, 2009] was based on seven Accelerator Mass Spectrometry (AMS) ^{14}C dates of the humic fraction of bulk organic matter which were calibrated into calendar ages using Calib 5.0 using a reservoir age of 1300 years. The *Proboscia* diatom counts were performed at a $\sim$10–20 years resolution. For the glycerol dibiphytanyl glycerol tetraether (GDGT) analysis, the sediment core was sampled on average at 180-year intervals. Sediments were freeze-dried, homogenized, and extracted as described by *Kim et al.* [2010].The extract was separated into an apolar, ketone, and polar fractions with Al$_2$O$_3$ column chromatography using hexane:DCM (9:1 v/v), hexane:DCM (1:1 v/v), and DCM:MeOH (1:1 v/v), respectively. The polar fractions were filtered using a 0.4 μm PTFE filter and analyzed with a high performance liquid chromatography-atmospheric pressure positive ionization-mass spectrometer (HPLC-APCI-MS) as described by *Schouten et al.*

[1]Department of Marine Organic Biogeochemistry, NIOZ Royal Netherlands Institute for Sea Research, Den Burg, Netherlands.
[2]EPOC, UMR 5805, Université de Bordeaux, Talence, France.
[3]Alfred Wegener Institute for Polar and Marine Research, Bremerhaven, Germany.
[4]Faculty of Earth and Life Sciences, Vrije Universiteit Amsterdam, Amsterdam, Netherlands.
[5]School of Natural Sciences, Edith Cowan University, Joondalup, Western Australia, Australia.
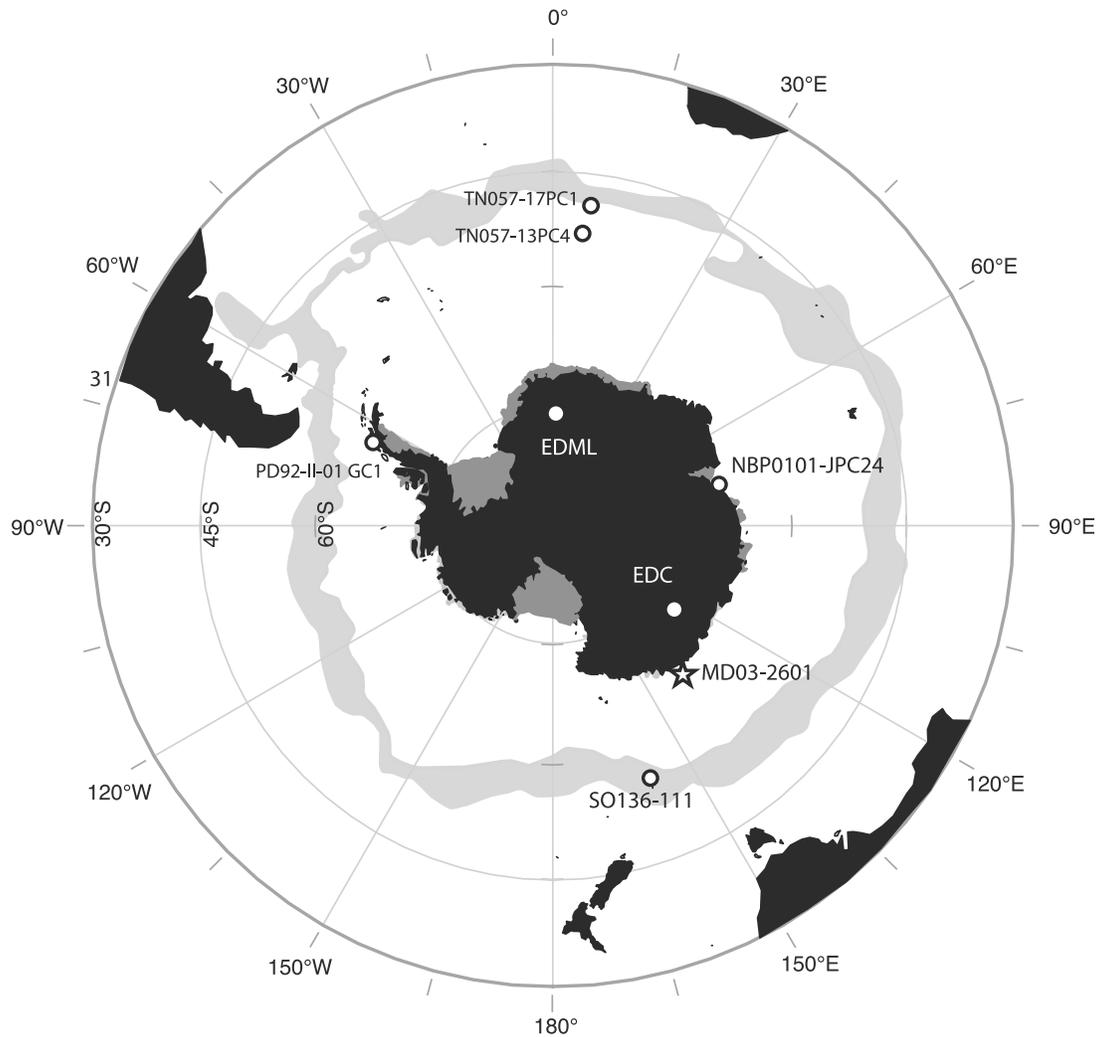
Figure 1. Core positions considered in this study: MD03-2601 [*Crosta et al.*, 2008], NBP0101-JPC24 [*Denis et al.*, 2010]. PD92-II-01 GC1 [*Taylor et al.*, 2001], TN057-17PC1 [*Nielsen et al.*, 2004], TN057-13PC4 [*Bianchi and Gersonde*, 2004], SO136-111 [*Crosta and Shemesh*, 2002], and EPICA ice cores drilled in Dronning Maud Land (EDML) and Dome C (EDC) [*Stenni et al.*, 2010].

[2007]. The TEX_{86}^L was calculated and converted into SSTs according to *Kim et al.* [2010]. All the samples were analyzed in duplicate with average analytical error being $\pm 0.2°C$ ($\pm 1\sigma$).

3. Results and Discussion

[4] TEX_{86}^L was developed based on the strong relationship between the distribution of thaumarchaeotal isoprenoid GDGTs and satellite-derived annual mean SST using a global core-top dataset [*Kim et al.*, 2010]. However, marine Thaumarchaeota, producing the membrane lipids used for TEX_{86}^L, occur throughout the whole water column [e.g., *Karner et al.*, 2001] and thus thaumarchaeotal GDGT-based temperature proxies may potentially integrate temperatures over a wide depth range (see auxiliary material). The TEX_{86}^L-derived temperatures may reflect predominantly epipelagic (approximately 0–200 m water depth on a global scale) temperatures because of the more efficient food web-based scavenging of thaumarchaeotal cells [e.g., *Wuchter et al.*, 2005]. Furthermore, Thaumarchaeota are virtually absent in the Antarctic summer surface water (the ∼0–45 m layer of low salinity water mass) in

contrast to their elevated abundances in winter in a ∼45–105 m interval of cold, salty water (i.e., the summer remnant of the previous winter, surface-mixed layer) [*Kalanetra et al.*, 2009]. Therefore, we hypothesize that TEX_{86}^L predominantly reflects subsurface (the depth interval ∼45–200 m) temperatures rather than SST. Consequently, we established a new calibration of TEX_{86}^L with depth-integrated annual mean temperatures from 0 to 200 m water depth (Figure 2). The calibration error is $\pm 2.8°C$, which is a systematic error, comprises many factors which are globally variable but at a single locality it will be of less importance or less variable [cf. *Tierney et al.*, 2010]. Thus, relative temperature variations within the TEX_{86}^L record will have a much lower error compared to absolute temperature estimates.

[5] Temperature reconstructed from TEX_{86}^L values of surface sediments derived from equation (S3) in Text S1 was on average 4.0°C (n = 2) at our core site, which is higher than the depth-integrated (0–200 m) annual mean temperature value of −0.2°C from the WOA09 [*Locarnini et al.*, 2010] but reasonable considering the calibration error. TEX_{86}^L-derived temperatures varied between 0°C and 4°C over the Holocene
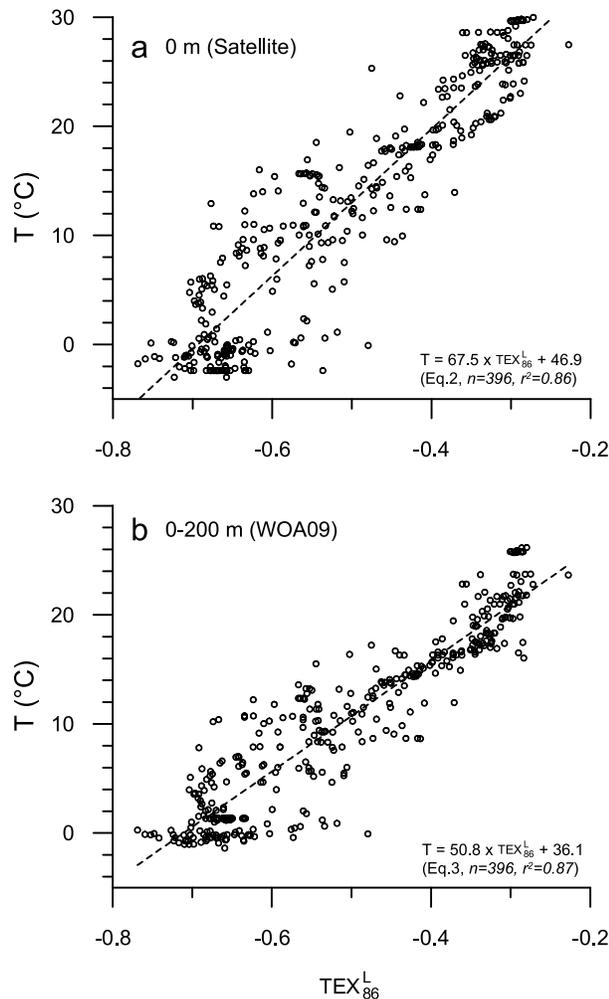
Figure 2. Comparison of TEX_{86}^L sediment core-top calibration models. (a) Cross plots of satellite SST with TEX_{86}^L values for the global calibration set (equation (S2) in Text S1) of *Kim et al.* [2010]. (b) Cross plots of depth-integrated annual mean WOA09 temperature for 0–200 m water depth [*Locarnini et al.*, 2010] with TEX_{86}^L values (equation (S3) in Text S1).

(Figure 3a). The most striking features of our TEX_{86}^L record are 1) a prominent increase in temperature centred at 6 kyr BP and 2) substantial temperature variability during the Late Holocene. Our TEX_{86}^L record (Figure 3a) does not show clear long-term cooling or warming trends which would be anticipated from orbitally driven insolation forcing (Figure 3b) [*Berger and Loutre*, 1991; *Renssen et al.*, 2005]. The TEX_{86}^L temperature variations also differ from those of temperature proxy records from other regions (Figure S3). In general, SH high-latitude records derived from diatom abundances (Figures S3a–S3c) infer a Mid Holocene warming and a subsequent cooling since 3–4 kyr BP for both the Antarctic Peninsula [*Taylor et al.*, 2001] and East Antarctica [*Denis et al.*, 2010]. In contrast, SH mid-latitude records [*Bianchi and Gersonde*, 2004; *Crosta and Shemesh*, 2002; *Nielsen et al.*, 2004] depict a general cooling until 4–5kyr BP (Figures S3d–S3f) and a subsequent warming (Figure S3d) or SST stabilization (Figure S3e). Temperature records inferred from Antarctic ice cores (Figures S3g and S3h) also demonstrate dissimilar Holocene variations

between sites (ΔT_{site}, SH high-latitude signals) and moisture sources (ΔT_{source}, SH mid-latitude signals) [*Stenni et al.*, 2010].

[6] To explore physical mechanisms associated with sub-surface temperature variability at our core site, we extracted anomalies of the annual mean temperatures of water masses at 30 m, 163 m, and 1225 m for the area 60–65°S, 135–145°E from the LOVECLIM coupled atmosphere–sea ice–ocean–vegetation model experiment, forced by annually varying orbital parameters, greenhouse gas concentrations, and Laurentide Ice Sheet deglaciation [*Renssen et al.*, 2010]. We selected these water depths in the model output because they provide a good representation of the surface-mixed layer, subsurface, and deep water masses, respectively. Surface and sub-surface simulated temperatures mimic Holocene climate evolution inferred from diatoms [*Crosta et al.*, 2008] while deep simulated temperatures are different than Holocene surface climate evolution. The simulated temperatures at all water depths (Figure 3c) show a pronounced peak at around 6 kyr BP in phase with a warming event recorded in the TEX_{86}^L record (Figure 3a). The reason for this pronounced maximum in the model calculation is that around 6 kyr BP, after complete recession of the Laurentide Ice Sheet, deep convection in the Labrador Sea became active, leading to greater North Atlantic Deep Water (NADW) flux and warmer NADW, which in turn warmed up Southern Ocean waters from below [*Renssen et al.*, 2010]. This warming of the deep water masses around 6 kyr BP is best seen in the simulated temperatures at 1225 m water depth (Figure 3c, blue curve). Return to cooler Southern Ocean conditions after 5.5 kyr BP was associated with the orbitally-forced cooling of the Southern Ocean and the source region of NADW in the Nordic and Labrador Seas [*Renssen et al.*, 2005, 2010]. Enhanced subsurface temperature variability during the Late Holocene as revealed by the TEX_{86}^L record is also apparent for the simulated surface and sub-surface temperatures but is less evident in simulated deep water temperatures. Poor representation of glacier dynamics and impacts in Antarctic coastal areas in the climate model for the Late Holocene on centennial time scales may have obscured variability of surface and sub-surface simulated temperatures [*Denis et al.*, 2009].

[7] For a coupling of subsurface temperature variability recorded by TEX_{86}^L (Figure 3a) with warmer, nutrient-rich MCDW intrusion at our core site comes from the Setae diatom group (S-DG; *Corethronpennatum, ChaetocerosPhaeoceros* spp., and *Rhizosolenia* spp. counts from *Denis et al.* [2010], Figure 3d) and the *Proboscia* spp. (*P. inermis, P. truncate,* and *P. alata,* Figure 3e, see also Figure S4; this study). Today, the S-DG group develops in summer and shows a clear preference for nutrient-rich, well-mixed waters in relation to katabatic winds [*Beans et al.*, 2008]. As intrusion of MCDW onto the continental shelf is induced by wind-induced Ekman pumping, the S-DG record at our core site probably indicates intensification of summer wind mixing and nutrient input since 3.5 kyr BP [*Denis et al.*, 2010]. The *Proboscia* spp. record in core MD03-2601 showed a similar long-term Holocene pattern with a general decrease between 10 and 5.5 kyr BP followed by an increase. This is in good agreement with a recent study in the western Antarctic Peninsula that, based on biomarkers for *Proboscia* diatoms showed increased *Proboscia* diatom productivity in shelf waters of the northwestern Antarctic Peninsula during the late Holocene in response to intensification of
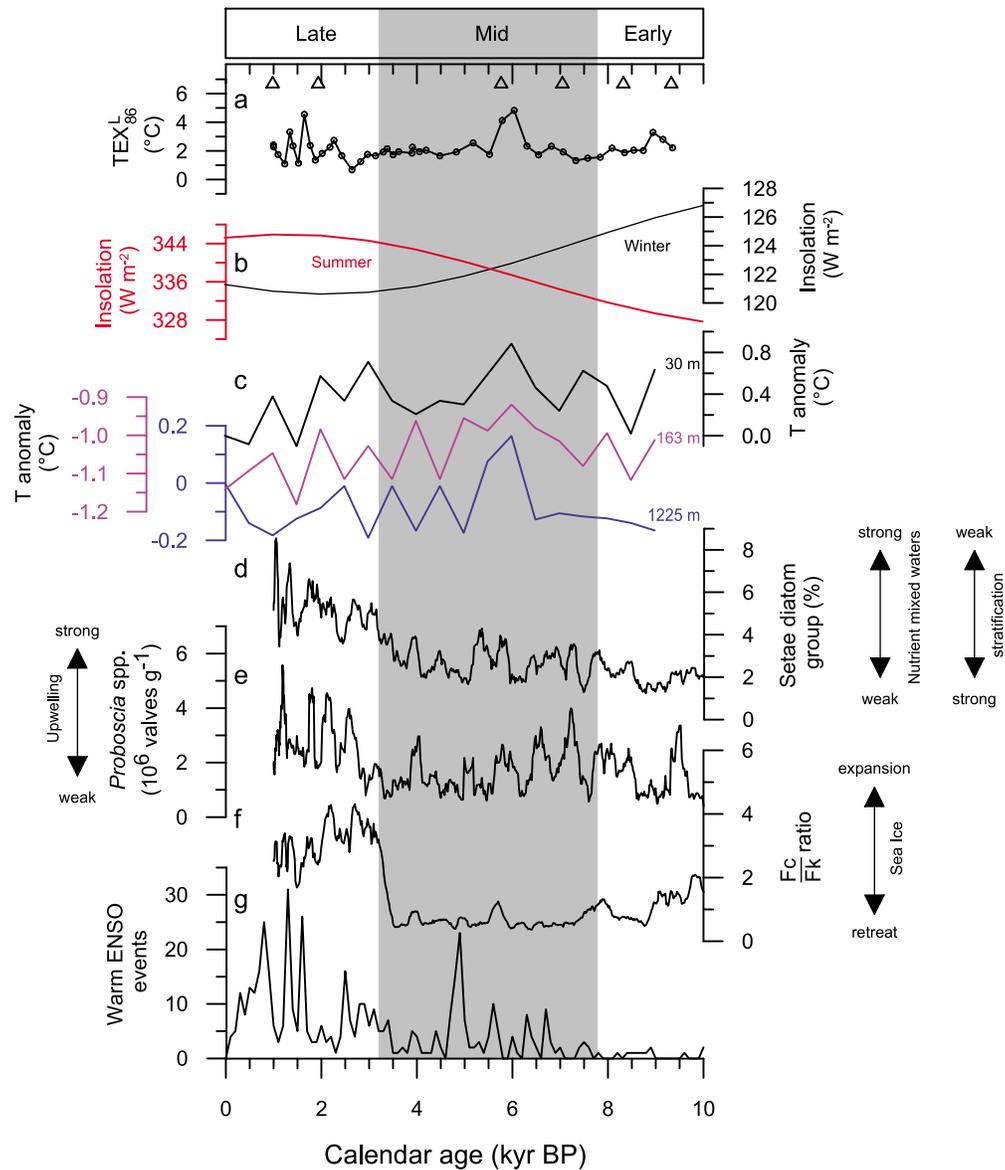
Figure 3. Comparison of Holocene climate record of MD03-2601 with modelled climate records. (a) TEX$_{86}^{L}$ temperature record from MD03-2601 using the 0–200 m core top calibration (equation (S3) in Text S1). Open triangles indicate the ^{14}C dating points. (b) Insolation changes at 60°S for summer (red line) and winter (black line) [*Berger and Loutre*, 1991]. (c) Simulated temperature anomalies calculated as deviations from the preindustrial mean (1000 − 250 yr BP) at 30 m (black line), 163 m (purple line), and 1225 m (blue line) water depth extracted from the area 60–65°S, 135–145°E (100-pointrunning mean) [*Renssen et al.*, 2010]. (d) Relative abundance of Setae diatom group (10-point running mean) [*Denis et al.*, 2010]. (e) Absolute abundance of *Proboscia* silica frustules. (f) Ratio between *Fragilariopsiscurta* and *Fragilariopsiskerguelensis* (Fc/Fk ratio, 10-point running mean) [*Denis et al.*, 2009]. (g) The number of warm ENSO events in 100-yr overlapping windows [*Moy et al.*, 2002].

MCDW upwelling [*Willmott et al.*, 2010]. This suggests that more frequent intensification of MCDW upwelling over the depth interval >∼100 m might have resulted in the observed warmer subsurface TEX$_{86}^{L}$ temperatures during the Late Holocene.

[8] Intriguingly, during the period of higher TEX$_{86}^{L}$-derived temperature variability (Figure 3a) and thus inferred more frequent, intensified intrusions of MCDW into the upper water column, sea ice over ice-free conditions during the growing season prevailed as shown by the ratio between *Fragilariopsis curta* and *Fragilariopsis kerguelensis* (Fc/Fk

ratio, Figure 3f) [*Denis et al.*, 2009]. This seemingly contradictory pattern between increased sea-ice cover and warmer temperature conditions during the Late Holocene can, however, be explained by the sea ice and temperature seasonal dynamics in the study area. The Late Holocene (i.e., Neoglacial period) was shown to experience greater late winter and early spring sea ice concentrations than the Mid Holocene (i.e., Hyperthermal period) [*Crosta et al.*, 2008; *Pike et al.*, 2009], which was favorable to the production of small *Fragilariopsis* species [*Beans et al.*, 2008]. After sea ice disintegration, more intense wind activity during summer

[*Steig et al.*, 2000; *van Ommen et al.*, 2004] may have promoted greater surface water mixing and upwelling of MCDW favorable to the production of S-DG [*Denis et al.*, 2010] and *Proboscia* diatom species. Upwelling of MCDW also resulted in warmer subsurface temperatures recorded in the TEX_{86}^L-derived temperature (Figure 3a).These sea ice and atmospheric seasonal dynamics have thus caused a simultaneous increase in sea ice related diatom (a spring record) and S-DG and *Proboscia* spp. (summer records) abundances during the Late Holocene at our core site.

[9] Our TEX_{86}^L record indicates that more frequent subsurface temperature changes with large amplitude at siteMD03-2601 was coincident with higher climate variability on a global scale during the Late Holocene [*Mayewski et al.*, 2004]. During this period, the ENSO conditions at low-latitudes [*Moy et al.*, 2002; *Cane*, 2005] were linked to orbitally induced changes in insolation seasonality (Figure 3g). The northward movement of the SH westerly wind belt with the reduction of zonal winds in its core zone in southernmost Chile [*Lamy et al.*, 2010] and abrupt fluctuations in sea temperature in the western Antarctic Peninsula [*Shevenell et al.*, 2011]are in good agreement with more El Niño-like conditions during the Late Holocene. Presently, low to high-latitude teleconnections are recognized in ENSO-sea ice relationships in the western Antarctic Peninsula region [*Stammerjohn et al.*, 2008]. Similarly, centennial-scale variability of subsurface temperatures in East Antarctica was probably coupled to the Late Holocene development of ENSO variability through wind variability along the eastern Antarctic coastal zone which impacted seasonal dynamics of upwelling intensity, SST, and sea ice extent. The proposed interaction between ENSO and subsurface conditions in East Antarctica should be further assessed with higher resolution TEX_{86}^L records.

4. Conclusions

[10] We present a Holocene ocean temperature record obtained from the eastern Antarctic continental margin using the archaeal membrane lipid-based paleothermometer (TEX_{86}^L) for the Polar Oceans. Our study showed that TEX_{86}^L-derived temperatures at our core site reflect a subsurface signal rather than surface. Interestingly, our TEX_{86}^L record does not show clear long-term cooling or warming trends but higher temperature variability during the Late Holocene. We hypothesise that this late Holocene temperature variability was linked to the intensification of MCDW intrusion onto the eastern Antarctic continental shelf in association with the centennial ENSO-like variability at low-latitudes. More TEX_{86}^L subsurface temperature records with higher temporal resolution will allow to elucidate the natural variability of MCDW intrusion to the inner continental shelf around Antarctica, which drives thinning and acceleration of glaciers [*Thoma et al.*, 2008] and will potentially further improve our knowledge of Antarctic ice sheet evolution, and its consequences for global environmental changes.

References

Beans, C., J. H. Hecq, P. Koubbi, C. Vallet, S. Wright, and A. Goffart (2008), A study of the diatom-dominated microplankton summer assemblages in coastal waters from Terre Adélie to the Mertz Glacier, East Antarctica (139°E–145°E), *Polar Biol.*, 31, 1101–1117, doi:10.1007/s00300-008-0452-x.

Berger, A., and M. F. Loutre (1991), Insolation values for the climate of the last 10 million years, *Quat. Sci. Rev.*, 10, 297–317, doi:10.1016/0277-3791(91)90033-Q.

Bianchi, C., and R. Gersonde (2004), Climate evolution at the last deglaciation: The role of the Southern Ocean, *Earth Planet. Sci. Lett.*, 228, 407–424, doi:10.1016/j.epsl.2004.10.003.

Bindoff, N. L., M. A. Rosenberg, and M. J. Warner (2000), On the circulation and water masses over the Antarctic continental slope and rise between 80 and 150E, *Deep Sea Res., Part II*, 47, 2299–2326, doi:10.1016/S0967-0645(00)00038-2.

Cane, M. A. (2005), The evolution of El Niño, past and future, *Earth Planet. Sci. Lett.*, 230, 227–240, doi:10.1016/j.epsl.2004.12.003.

Crosta, X., and A. Shemesh (2002), Reconciling down core anticorrelation of diatom carbon and nitrogen isotopic ratios from the Southern Ocean, *Paleoceanography*, 17(1), 1010, doi:10.1029/2000PA000565.

Crosta, X., D. Denis, and O. Ther (2008), Sea ice seasonality during the Holocene, Adélie Land, East Antarctica, *Mar. Micropaleontol.*, 66, 222–232, doi:10.1016/j.marmicro.2007.10.001.

Denis, D., et al. (2009), Holocene glacier and deep water dynamics, Adélie Land, East Antarctica, *Quat. Sci. Rev.*, 28, 1291–1303, doi:10.1016/j.quascirev.2008.12.024.

Denis, D., X. Crosta, L. Barbara, G. Massé, H. Renssen, O. Ther, and J. Giraudeau (2010), Sea ice and wind variability during the Holocene in East Antarctica: Insight on middle high latitude coupling, *Quat. Sci. Rev.*, 29, 3709–3719, doi:10.1016/j.quascirev.2010.08.007.

Hodell, D., S. L. Kanfoush, A. Shemesh, X. Crosta, C. D. Charles, and T. P. Guilderson (2001), Abrupt cooling of Antarctic surface waters and sea ice expansion in the South Atlantic sector of the Southern Ocean at 5000 cal yr B.P., *Quat. Res.*, 56, 191–198, doi:10.1006/qres.2001.2252.

Kaiser, J., E. Schefuß, F. Lamy, M. Mohtadi, and D. Hebbeln (2008), Glacial to Holocene changes in sea surface temperature and coastal vegetation in north central Chile: High versus low latitude forcing, *Quat. Sci. Rev.*, 27, 2064–2075, doi:10.1016/j.quascirev.2008.08.025.

Kalanetra, K. M., N. Bano, and J. T. Hollibaugh (2009), Ammonia-oxidizing Archaea in the Arctic Ocean and Antarctic coastal waters, *Environ. Microbiol.*, 11, 2434–2445, doi:10.1111/j.1462-2920.2009.01974.x.

Karner, M. B., E. F. DeLong, and D. M. Karl (2001), Archaeal dominance in the mesopelagic zone of the Pacific Ocean, *Nature*, 409, 507–510, doi:10.1038/35054051.

Kim, J.-H., S. van der Meer, S. Schouten, P. Helmke, V. Willmott, F. Sangiorgi, N. Koç, E. C. Hopmans, and J. S. Sinninghe Damsté (2010), New indices and calibrations derived from the distribution of crenarchaealisoprenoidtetraether lipids: Implications for past sea surface temperature reconstructions, *Geochim. Cosmochim. Acta*, 74, 4639–4654, doi:10.1016/j.gca.2010.05.027.

Lacarra, M., M.-N. Houssais, E. Sultan, S. R. Rintoul, and C. Herbaut (2011), Summer hydrography on the shelf off Terre Adélie/George V Land based on the ALBION and CEAMARC observations during the IPY, *Polar Sci.*, 5, 88–103, doi:10.1016/j.polar.2011.04.008.

Lamy, F., R. Kilian, H. W. Arz, J.-P. Francois, J. Kaiser, M. Prange, and T. Steinke (2010), Holocene changes in the position and intensity of the southern westerly wind belt, *Nat. Geosci.*, 3, 695–699, doi:10.1038/ngeo959.

Locarnini, R. A., A. V. Mishonov, J. I. Antonov, T. P. Boyer, H. E. Garcia, O. K. Baranova, M. M. Zweng, and D. R. Johnson (2010), *World Ocean Atlas 2009*, vol. 1, *Temperature*, NOAA Atlas NESDIS, vol. 68, edited by S. Levitus, 184 pp., NOAA, Silver Spring, Md.

Mayewski, P. A., et al. (2004), Holocene climate variability, *Quat. Res.*, 62, 243–255, doi:10.1016/j.yqres.2004.07.001.

Moy, C. M., G. O. Seltzer, D. T. Rodbell, and D. M. Anderson (2002), Variability of El Niño/Southern Oscillation activity at millennial timescales during the Holocene epoch, *Nature*, 420, 162–165, doi:10.1038/nature01194.

Nielsen, S. H. H., N. Koç, and X. Crosta (2004), Holocene climate in the Atlantic sector of the Southern Ocean: Controlled by insolation or oceanic circulation?, *Geology*, 32, 317–320, doi:10.1130/G20334.1.

Pike, J., X. Crosta, E. J. Maddison, C. E. Stickley, D. Denis, L. Barbara, and H. Renssen (2009), Observations on the relationship between the Antarctic coastal diatoms *Thalassiosiraant arctica* Comber and *Porosira glacialis* (Grunow) Jørgensen and sea ice concentrations during the Late Quaternary, *Mar. Micropaleontol.*, 73, 14–25, doi:10.1016/j.marmicro.2009.06.005.

Renssen, H., H. Goosse, T. Fichefet, V. Masson-Delmotte, and N. Koç (2005), The Holocene climate evolution in the high-latitude Southern Hemisphere simulated by a coupled atmosphere-sea ice-ocean-vegetation model, *Holocene*, 15, 951–964, doi:10.1191/0959683605hl869ra.

Renssen, H., H. Goosse, X. Crosta, and D. M. Roche (2010), Early Holocene Laurentide Ice Sheet deglaciation causes cooling in the high-latitude Southern Hemisphere through oceanic teleconnection, *Paleoceanography*, 25, PA3204, doi:10.1029/2009PA001854.

Schouten, S., E. C. Hopmans, E. Schefuß, and J. S. Sinninghe Damsté (2002), Distributional variations in marine crenarchaeotal membrane lipids: A new organic proxy for reconstructing ancient sea water temperatures?, *Earth Planet. Sci. Lett.*, 204, 265–274, doi:10.1016/S0012-821X (02)00979-2.

Schouten, S., C. Huguet, E. C. Hopmans, M. Kienhuis, and J. S. Sinninghe Damsté (2007), Analytical methodology for TEX$_{86}$ paleothermometry by high-performance liquid chromatography/atmospheric pressure chemical ionization-mass spectrometry, *Anal. Chem.*, 79, 2940–2944, doi:10.1021/ac062339v.

Shevenell, A. E., A. E. Ingalls, E. W. Domack, and C. Kelly (2011), Holocene Southern Ocean surface temperature variability west of the Antarctic Peninsula, *Nature*, 470, 250–254, doi:10.1038/nature09751.

Stammerjohn, S. E., D. G. Martinson, R. C. Smith, X. Yuan, and D. Rind (2008), Trends in annual sea ice retreat and advance and their relation to El Niño-Southern Oscillation and Southern Annular Mode variability, *J. Geophys. Res.*, 113, C03S90, doi:10.1029/2007JC004269.

Steig, E. J., D. L. Morse, E. D. Waddington, M. Stuiver, P. M. Grootes, P. A. Mayewski, M. S. Twickler, and S. I. Whitlows (2000), Wisconsinan and Holocene climate history from an ice core at Taylor Dome, western Ross Embayment, Antarctica, *Geogr. Ann., Ser. A*, 82, 213–235, doi:10.1111/j.0435-3676.2000.00122.x.

Stenni, B., et al. (2010), The deuterium excess records of EPICA Dome C and Dronning Maud Land ice cores (East Antarctica), *Quat. Sci. Rev.*, 29, 146–159, doi:10.1016/j.quascirev.2009.10.009.

Taylor, F., J. Whitehead, and E. Domack (2001), Holocene paleoclimate change in the Antarctic Peninsula: Evidence from the diatom, sedimentary and geochemical record, *Mar. Micropaleontol.*, 41, 25–43, doi:10.1016/S0377-8398(00)00049-9.

Thoma, M., A. Jenkins, D. Holland, and S. Jacobs (2008), Modelling Circumpolar Deep Water intrusions on the Amundsen Sea continental shelf, Antarctica, *Geophys. Res. Lett.*, 35, L18602, doi:10.1029/2008GL034939.

Tierney, J. E., M. T. Mayes, N. Meyer, C. Johnson, P. W. Swarzenski, A. S. Cohen, and J. M. Russell (2010), Late twentieth-century warming in Lake Tanganyika unprecedented since AD 500, *Nat. Geosci.*, 3, 422–425, doi:10.1038/ngeo865.

van Ommen, T. D., V. I. Morgan, and M. A. J. Curran (2004), Deglacial and Holocenechanges in accumulation at Law Dome, *Ann. Glaciol.*, 39, 359–365, doi:10.3189/172756404781814221.

Williams, G. D., S. Aoki, S. S. Jacobs, S. R. Rintoul, T. Tamura, and N. L. Bindoff (2010), Antarctic bottom water from Adélie and George V Land Coast, East Antarctica, *J. Geophys. Res.*, 115, C04027, doi:10.1029/2009JC005812.

Willmott, V., S. W. Rampen, E. Domack, M. Canals, J. S. Sinninghe Damsté, and S. Schouten (2010), Holocene changes in Proboscia diatom productivity in shelf waters of the north-western Antarctic Peninsula, *Antarct. Sci.*, 22, 3–10, doi:10.1017/S095410200999037X.

Wuchter, C., S. Schouten, S. G. Wakeham, and J. S. Sinninghe Damsté (2005), Temporal and spatial variation in tetraether membrane lipids of marine Crenarchaeota in particulate organic matter: Implication for TEX$_{86}$ paleothermometry, *Paleoceanography*, 20, PA3013, doi:10.1029/2004PA001110.

J. Bonnin and X. Crosta, EPOC, UMR 5805, Université de Bordeaux, 1, Avenue des Facultés, F-33405 Talence CEDEX, France.

P. Helmke, School of Natural Sciences, Edith Cowan University, 270 Joondalup Dr., Joondalup, WA 6027, Australia.

J.-H. Kim, S. Schouten, and J. S. Sinninghe Damsté, Department of Marine Organic Biogeochemistry, NIOZ Royal Netherlands Institute for Sea Research, PO Box 59, NL-1790 AB Den Burg, Netherlands. (jung-hyun.kim@nioz.nl)

H. Renssen, Faculty of Earth and Life Sciences, Vrije Universiteit Amsterdam, De Boelelaan 1085, NL-1081 HV Amsterdam, Netherlands.

V. Willmott, Alfred Wegener Institute for Polar and Marine Research, Am Handelshafen 12, D-27570 Bremerhaven, Germany.